

TABLE OF CONTENTS



TABLE OF CONTENTS

	Page
1.0 CONVENTIONAL CORE ANALYSIS	i-ii
1.1 Inventory of Whole Core	1
1.2 Total Gamma Ray Analysis	1
1.3 Conventional Core Description and Photography	5
1.4 Drilled Plugs and Routine Core Analysis	5
2.0 GEOLOGICAL CHARACTERIZATION	10
2.1 Introduction	10
2.2 Core Description	10
2.3 Description of Reservoir Zones	12
2.4 X-Ray Diffraction Analysis	16
3.0 WELLSITY FIELD SERVICES AND DESORPTION	21
3.1 Introduction and Procedures	21
3.2 Results	22
4.0 LABORATORY DESORPTION	24
4.1 Long-Term Desorption	24
4.2 Headspace	24
4.3 Residual Gas	24
4.4 Results	24
5.0 TOTAL ORGANIC CARBON (TOC) AND ROCK EVAL	33
5.1 Introduction and Procedures	33
5.2 Results	33
6.0 EXTENDED GAS ANALYSIS	35
6.1 Introduction and Procedures	35
6.2 Results	35

Tables

Table 1.1 Total Gamma Log	2-3
Table 1.2 Routine Properties Sample Inventory	7
Table 1.3 Summary of Routine Core Analysis Results	8
Table 2.1 Analyses Performed	17
Table 2.2 Thin Section Analysis	18-19
Table 2.3 X-Ray Diffraction Analysis	20
Table 3.1 Inventory of Recovered Coal and Canisters	22
Table 3.2 Summary of Shale Gas Properties	23
Table 5.1 TOC and Rock Eval Data Report	34

Figures

Figure 1.1	Gamma, Permeability and Porosity Plot	4
Figure 1.2	Routine Properties Permeability vs. Porosity	9
Figure 4.1	Cumulative Gas Desorbed, Canister #1	26
Figure 4.2	Cumulative Gas Desorbed, Canister #2	27
Figure 4.3	Cumulative Gas Desorbed, Canister #3	28
Figure 4.4	Cumulative Gas Desorbed, Canister #4	29
Figure 4.5	Cumulative Gas Desorbed, Canister #5	30
Figure 4.6	Cumulative Gas Desorbed, Canister #6	31
Figure 4.7	Cumulative Gas Desorbed, Canister #7	32

APPENDICES

- APPENDIX A – Conventional Core Photography Report**
- APPENDIX B – Conventional Core Description**
- APPENDIX C – Thin Section Description and Photomicrographs**
- APPENDIX D – Desorption and Proximate Analysis Data**
- APPENDIX E – TOC / Rock-Eval Data**
- APPENDIX F – Extended Gas Analysis Data**

1.0 CONVENTIONAL CORE ANALYSIS

1.1 Inventory of Whole Core

Routine Core Analysis, including Gamma Log Analysis was performed on cores representing the 6666.0 - 6763.6 foot intervals of the Hunton Formation from the Fowler #2-17 Well. During coring seven, three foot sections of the Woodford Formation were taken for desorption testing.

1.2 Total Gamma Ray Analysis

Procedure and Introduction

A detailed Total Gamma Log Analysis was performed on cores representing the 6666.0 - 6763.6 foot intervals of the Hunton Formation. The desorbed sections of these cores were not analyzed for total gamma radiation.

The whole core was placed on the conveyer belt and was moved through the Temco SGL 891 Spectral Gamma logger, which measures total gamma radiation, at a constant rate of 2 to 5 feet per minute with a depth resolution of about 6 inches. During this process the core was evaluated for shale and non-shale quantities and these quantities were converted to standard gamma ray log API units. Total gamma API values in the lower range represent little to no shale present. Conversely, total gamma API values in the higher range represent mostly shale present. These values are then plotted against the specific core depths at which they are obtained. Total Gamma Log data are represented in both tabular and graphic formats below.

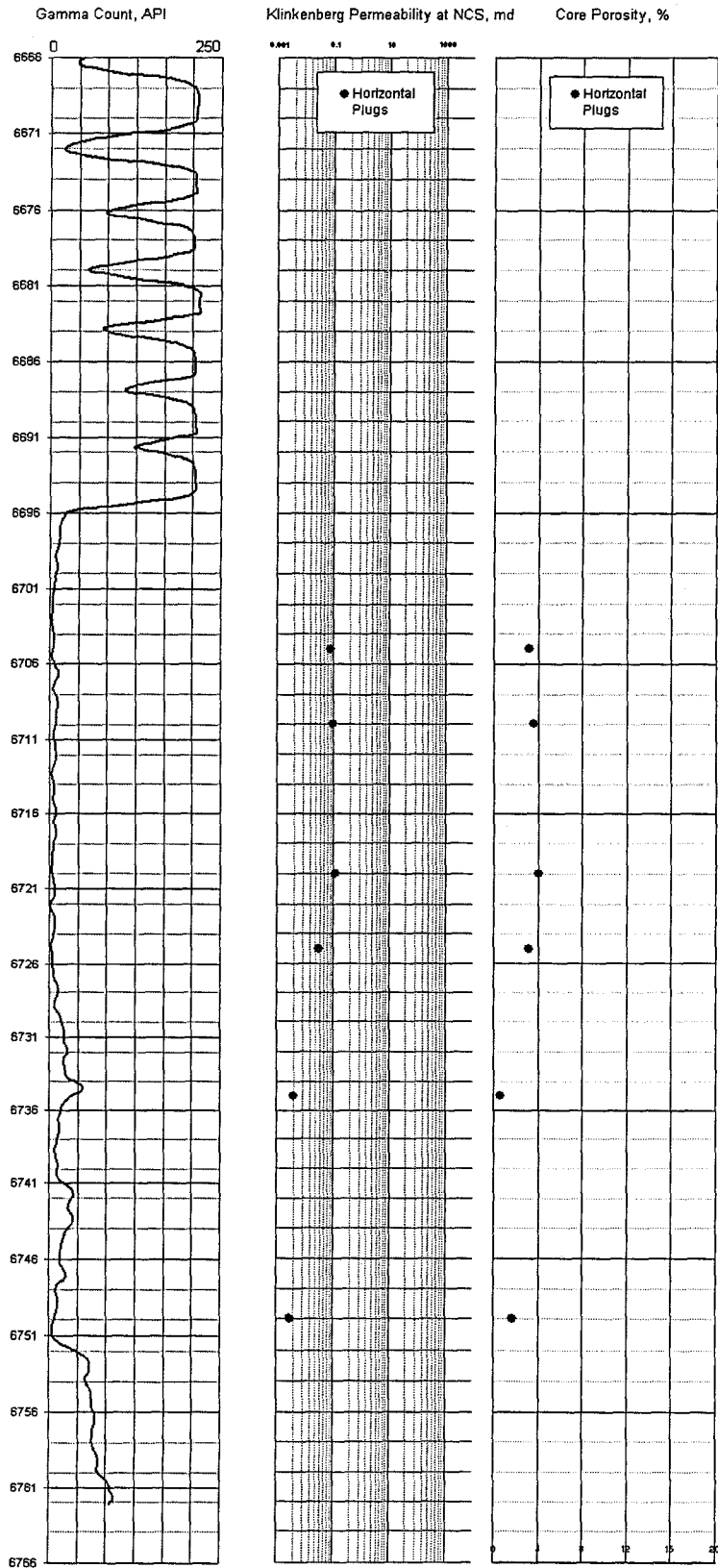
Table 1.1. Total Gamma Log

Depth (ft)	Total Gamma						
6666.00	57.6	6689.35	253.2	6712.70	7.6	6736.05	21.3
6666.47	49.1	6689.82	255.0	6713.17	3.7	6736.52	17.1
6666.93	107.0	6690.28	255.6	6713.63	5.4	6736.98	18.6
6667.40	210.3	6690.75	255.3	6714.10	8.9	6737.45	18.0
6667.87	249.6	6691.22	190.7	6714.57	8.7	6737.92	13.5
6668.34	257.6	6691.68	147.4	6715.03	6.6	6738.38	12.3
6668.80	259.2	6692.15	205.0	6715.50	10.9	6738.85	10.4
6669.27	256.4	6692.62	247.1	6715.97	12.6	6739.32	12.4
6669.74	256.5	6693.09	253.6	6716.44	8.2	6739.79	15.9
6670.20	254.3	6693.55	255.3	6716.90	10.0	6740.25	14.4
6670.67	209.4	6694.02	255.9	6717.37	11.6	6740.72	17.8
6671.14	114.6	6694.49	256.0	6717.84	9.0	6741.19	33.8
6671.60	45.2	6694.95	235.5	6718.30	7.1	6741.65	43.2
6672.07	24.5	6695.42	134.1	6718.77	6.2	6742.12	37.0
6672.54	79.8	6695.89	38.3	6719.24	6.6	6742.59	33.3
6673.00	190.1	6696.35	21.5	6719.70	4.6	6743.05	39.9
6673.47	248.8	6696.82	17.4	6720.17	5.3	6743.52	42.3
6673.94	254.6	6697.29	17.5	6720.64	8.4	6743.99	32.4
6674.41	254.7	6697.76	16.5	6721.11	10.4	6744.46	25.4
6674.87	255.9	6698.22	13.6	6721.57	8.4	6744.92	22.2
6675.34	221.5	6698.69	10.3	6722.04	2.8	6745.39	21.3
6675.81	129.4	6699.16	11.4	6722.51	3.7	6745.86	20.9
6676.27	97.6	6699.62	14.2	6722.97	9.4	6746.32	19.6
6676.74	176.5	6700.09	10.2	6723.44	10.6	6746.79	28.0
6677.21	240.0	6700.56	8.4	6723.91	9.1	6747.26	27.5
6677.67	251.5	6701.02	8.6	6724.37	5.8	6747.72	14.1
6678.14	254.3	6701.49	6.2	6724.84	4.5	6748.19	13.1
6678.61	249.7	6701.96	5.7	6725.31	6.2	6748.66	15.6
6679.08	206.1	6702.43	5.5	6725.78	7.0	6749.13	16.5
6679.54	116.6	6702.89	4.4	6726.24	6.7	6749.59	12.8
6680.01	67.6	6703.36	5.1	6726.71	7.7	6750.06	8.8
6680.48	137.1	6703.83	6.1	6727.18	11.0	6750.53	6.8
6680.94	231.2	6704.29	8.6	6727.64	15.6	6750.99	6.3
6681.41	261.4	6704.76	7.4	6728.11	14.5	6751.46	19.2
6681.88	260.9	6705.23	4.8	6728.58	10.3	6751.93	45.0
6682.34	261.1	6705.69	6.5	6729.04	10.5	6752.39	63.1
6682.81	262.5	6706.16	10.8	6729.51	18.2	6752.86	70.5
6683.28	192.0	6706.63	15.3	6729.98	22.9	6753.33	70.2
6683.75	94.2	6707.10	9.2	6730.45	25.6	6753.80	62.0
6684.21	121.7	6707.56	5.9	6730.91	25.4	6754.26	67.9
6684.68	209.2	6708.03	11.3	6731.38	25.6	6754.73	75.7
6685.15	245.2	6708.50	14.3	6731.85	31.9	6755.20	74.6
6685.61	252.9	6708.96	13.0	6732.31	26.4	6755.66	75.5
6686.08	254.7	6709.43	11.5	6732.78	25.4	6756.13	80.4
6686.55	255.5	6709.90	11.4	6733.25	28.8	6756.60	80.9
6687.01	246.0	6710.36	8.3	6733.71	32.7	6757.06	77.8
6687.48	162.1	6710.83	9.0	6734.18	53.8	6757.53	76.7
6687.95	132.0	6711.30	10.4	6734.65	56.6	6758.00	75.7
6688.42	208.0	6711.77	10.7	6735.12	34.6	6758.47	79.1
6688.88	245.9	6712.23	11.8	6735.58	24.6	6758.93	85.8

Table 1.1. Total Gamma Log (Continued)

Depth (ft)	Total Gamma
6759.40	87.0
6759.87	84.4
6760.33	94.7
6760.80	104.6
6761.27	107.0
6761.73	114.3
6762.20	106.2
6762.669	88.3
6763.136	59.1
6763.603	24.9

Figure 1.1. Gamma, Permeability and Porosity Plot



1.3 Conventional Core Descriptions and Photography

The core description serves as a permanent record useful for future engineering or geological studies. The core description was conducted for the express purpose of defining the core's lithology, depositional features, structural elements, core damage and core orientation. The conventional core description is essential because visual records will permit inspection of rock features and textures if the core is inaccessible or destroyed. The core description, in full color, is located in Appendix B in the back of this report.

Core Photographs were taken after the core had been slabbed to improve clarity and maximize the exposure of depositional features and rock fabric. A continuous (composite) core photograph format was used in which the core is generally photographed in 3 foot intervals. The core photographs are located in Appendix A in the back of this report.

1.4 Drilled Plugs and Routine Core Analysis

Introduction and Procedure

A total of 6 plugs were drilled from whole core not including the desorbed sections.

The properties of fluid saturation, porosity and permeability are commonly referred to as Routine Core Analysis. These properties are often the most important parameters in reservoir evaluation. Also, included in Routine Core Analysis are general sample descriptions. All of these properties together aim to reflect in-situ reservoir properties.

In order for reliable core analysis results to be measured the samples must first go through a preparation process. The 6 samples from the Fowler #2-17 well were thoroughly cleaned of reservoir liquids and drilling fluids prior to standard measurements of porosity and permeability using the Dean Stark Distillation Extraction Method. The samples were first weighed then placed into the Dean Stark apparatus. The solvent Toluene is vaporized by boiling. The Toluene rises around and through the core, is condensed and remains in a continuous reflux over the sample until all the water has been collected in a calibrated receiving tube. The collected water volume is then recorded to obtain the residual water saturation of the core. Dean Stark extraction is then followed by soxhlet extraction with methanol to remove salts from the sample. The samples were then dried in a vacuum oven to remove any remaining water and solvent. Samples were dried to a stable weight and this weight is recorded.

The properties of fluid saturation, porosity and permeability of the core sample were then obtained through basic core analysis. Fluid saturation was calculated using data from the Dean Stark method of Distillation and Extraction. Gas Permeability and porosity were measured using the Coretest AP-608, which allows rotary core samples to be measured under realistic reservoir conditions. Permeability measurements were made using an unsteady-state pulse decay technique at minimum confining stress.

Porosity and pore volume were measured using helium expansion based on Boyle's Law. Helium grain volume was also measured at ambient conditions. The cores were then described by geologist for the express purpose of defining lithology, depositional features, core damage, and structural and diagenetic elements.

Results

The following Table 1.2 is a sample inventory of all the samples designated for Routine Properties Testing. On the following pages, Table 1.3 lists the permeability and porosity results from the testing and Figure 1.1 illustrating the plot of permeability vs. porosity.

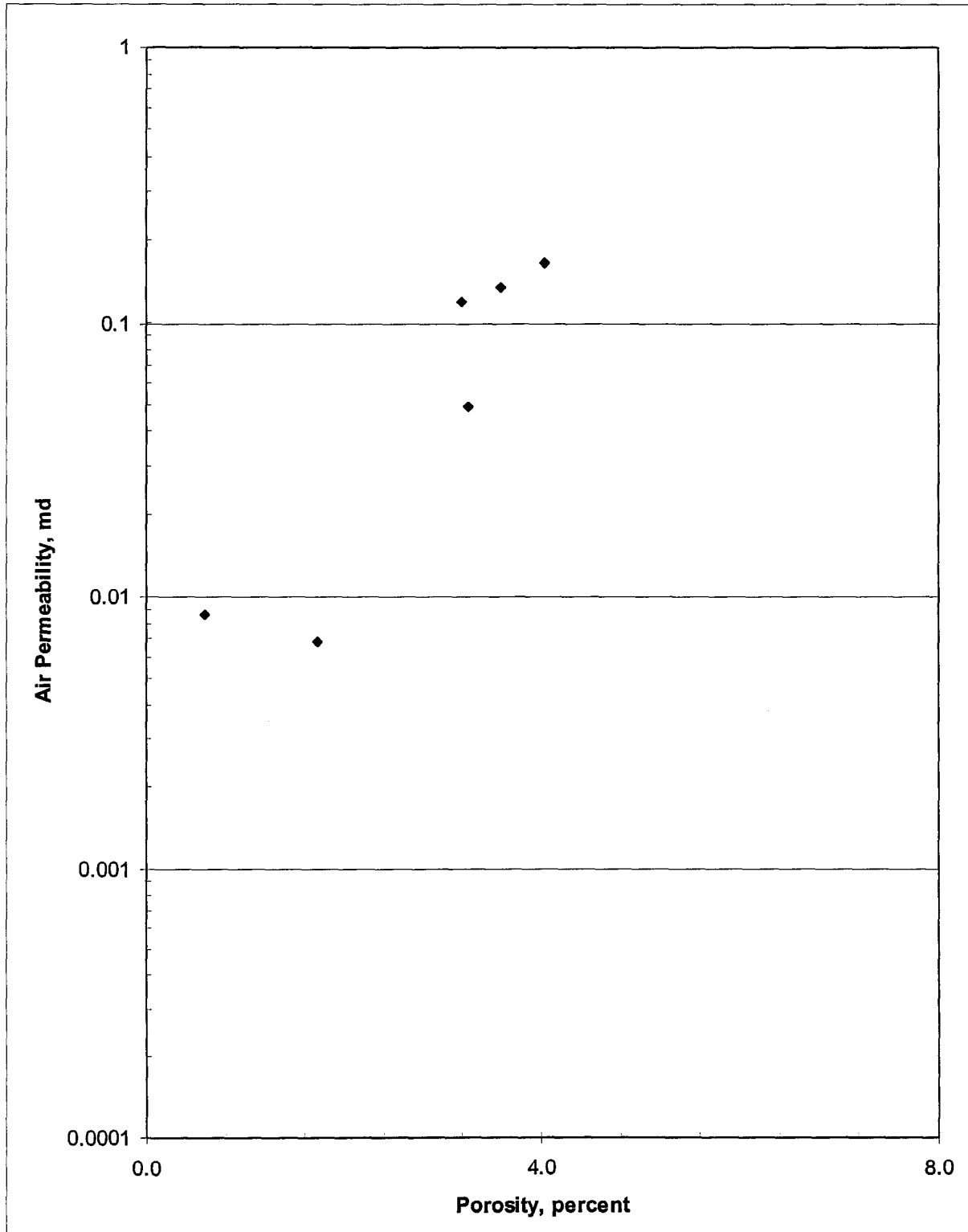
Table 1.2. Routine Properties Sample Inventory

Sample ID	Depth (ft)	Well Name	Remarks	Routine Properties			
				Dean-Stark Saturation	Grain Vol / Den	Pore Vol / Porosity	Air Perm
2	6705.0	Fowler #2-17		X	X	X	X
4	6710.0	Fowler #2-17		X	X	X	X
6	6720.0	Fowler #2-17		X	X	X	X
7	6725.0	Fowler #2-17		X	X	X	X
9	6735.0	Fowler #2-17		X	X	X	X
11	6750.0	Fowler #2-17		X	X	X	X

Table 1.3. Summary of Routine Core Analysis Results

Sample ID	Depth	Net	Dry	Length (cm)	Diameter (cm)	Grain Volume (cm ³)	Grain Density (g/cm ³)	Pore Volume (cm ³)	Bulk Volume (cm ³)	Porosity (percent)	Air Permeability (md)	Klinkenberg	Pore Volume Saturations			Lithological Description
		Confining Stress (psi)	Weight (g)									Air Permeability (md)	Water %	Oil %	Gas %	
2	6705.0	800	52.020	4.120	2.470	18.940	2.747	0.622	19.562	3.2	0.121	0.0848	24.4	0.00	75.6	Limestone, lt-med gray, recrystallized, skeletal frag, small intrxn pores, bitu
4	6710.0	800	65.210	5.188	2.476	23.870	2.732	0.889	24.759	3.6	0.135	0.100	22.7	0.0	77.3	Limestone, med gray, rexized, skel frag, pin-point vugs, interxln pores, bitur
6	6720.0	800	65.590	5.175	2.483	23.830	2.752	1.002	24.832	4.0	0.165	0.125	50.4	0.0	49.6	Limestone, lt-med gray, skel frag, pin point vugs, interxln pores, minor bitum
7	6725.0	800	59.330	4.630	2.480	21.600	2.747	0.726	22.326	3.3	0.049	0.034	34.8	0.0	65.2	Limestone, lt gray, f xln, pack-wackestone, pel, skel, styl, minor bitumen
9	6735.0	800	54.600	4.190	2.490	20.020	2.727	0.120	20.140	0.6	0.0087	0.0041	36.1	0.0	63.9	Limestone, lt-med gray, pel, skel, packstone, tight, spar cement
11	6750.0	800	55.680	4.370	2.469	20.460	2.721	0.359	20.819	1.7	0.0069	0.0032	14.1	0.0	85.9	Limestone, med gray, echinoderm grainstone, compacted, spar cement

Figure 1.2. Routine Properties Permeability vs. Porosity



2.0 GEOLOGICAL CHARACTERIZATION

2.1 Introduction

A detailed geologic description was performed on approximately 91 feet of slabbed core from the Sedna Energy Fowler No. 2-17 well, Haskell County, Oklahoma (Figure 1). The core examined represents the 6666-6765 foot interval in this well (core depths). The described interval represents the Woodford Shale (6666.0-6696.0 ft) and the Hunton Limestone (6696-6765.0 ft). A number of 1-foot long sections of the Woodford Shale were removed prior to slabbing and geologic description. The geologic description was supplemented with a modest amount of petrography. Three (3) thin sections from the Woodford Shale zone and ten (10) thin sections from the Hunton Limestone zone were prepared and analyzed. Additionally, six (6) samples from the Hunton Limestone zone were subjected to bulk x-ray diffraction techniques. Table 1 lists specific depths and analyses performed.

Analytical Methods

End pieces trimmed from six (6) 1-inch diameter plugs drilled from conventional cores as well as thin billets cut from the back side of the slabbed core were vacuum impregnated with fluorescent red (rhodamine) epoxy resin, surfaced, mounted on a glass slide and polished to a thickness of approximately 30 μm . The resulting thin sections were stained with a combination of alizarin red "S" and potassium ferricyanide to aid in identification of carbonate minerals. Thin sections were examined and photographed using a Zeiss Universal petrographic microscope. Petrographic analysis of thin sections yielded qualitative information concerning rock texture, composition, cementation, diagenesis, reservoir quality and pore geometry. The results of thin section analysis are presented in Table 2. Plane (color) and ultraviolet light photomicrographs are presented as a series of plates in the back of this report.

A portion of six (6) samples was analyzed by x-ray diffraction. A small piece of material trimmed from the end of drilled core plugs was ground to a fine powder ($\sim 2\text{-}5\ \mu\text{m}$) with a McCrone mill, back-loaded into an aluminum sample holder and scanned with a Philips x-ray diffractometer from 2 to 60 degrees 2-theta with copper Ka radiation. The resulting diffractogram was interpreted using APD and ProFit software yielding a semi-quantitative weight percentage of bulk rock mineralogy (total clay, quartz, feldspars, calcite, dolomite, pyrite, etc.). Bulk x-ray diffraction analysis data are presented in Table 3.

2.2 Core Description

Woodford Shale - The upper 30 feet of recovered core (6666-6696 ft) represents the Woodford Shale. The slabbed core contains a number of missing sections that were removed for desorption and other testing. These rocks are characterized as thinly laminated, organic-rich, black shale. The upper portion contains thin interlaminae

composed of radiolarian chert. Small amounts of terrigenous and skeletal debris as well as pyrite and pyritized shell fragments are present along some laminae. Thin chert laminae range up to 1.5 cm in thickness, but most are on a millimeter scale. Narrow mineralized fractures (dolomite-filled) are present within some chert laminae. Fractures exhibit very little natural porosity.

The lower portion of the Woodford zone contains fewer chert interbeds and is dominated by organic-rich shale. Small amounts of pyrite and skeletal debris are present along some laminae. Several shear fractures containing slickensides were observed in this zone. Thin section analysis of shear fractures indicates that minor amounts of calcite are present along fracture traces. The contact between the Woodford zone and underlying Hunton Limestone was not visible in the core, but is characterized elsewhere as erosional. The Woodford zone was deposited in relatively deep water over the karsted top surface of the Hunton Limestone.

Hunton Limestone - The Hunton Limestone is divided into several units. The upper portion of the core is characterized by partial dolomitization. The contact with the Woodford shale is an unconformity and is likely karsted. The upper portion of the Hunton Limestone is characterized by light gray, moderately dolomitized limestone. Dolomitization has destroyed much of the original texture. Only selected skeletal grains remain undolomitized. Hints of the original texture suggest that these rocks were originally crinoidal packstones.

Rocks underlying the partially dolomitized section are characterized as skeletal packstones to wackestones. These rocks have a micrite matrix. Biotic diversity is much greater in this undolomitized section. Skeletal grains include echinoderms, brachiopods, bryozoans, ostracods, trilobites and tabular skeletal grains. The packstone to wackestone interval extends from approximately 6725-6750 ft. One thin zone located at approximately 6742 ft exhibits a microkarst solution cavity filled by internal sediment.

A thin zone from approximately 6749.5-6751.5 ft is characterized as a skeletal grainstone. This interval contains abundant skeletal and non-skeletal grains cemented by calcite spar. Skeletal components include echinoderms, green algal fragments, algal coated grains and brachiopod fragments. Non-skeletal grains are a mixture of ooids and intraclasts. This interval has a sharp base and probably represents the highest energy deposit in the cored interval.

The lower portion of the cored interval is characterized by light green and dark gray shale. A thin transition zone of shaly limestone separates the Hunton Limestone from the shale interval. The interval from 6752.5-6762 ft is composed of light green shale. The interval from 6762-6765 ft is composed of dark gray shale. The contact between the shaly units is diagenetic rather than stratigraphic. Green shales have been chemically reduced, whereas dark gray shales have been oxidized.

2.3 Description of Reservoir Zones

Woodford Shale

The three (3) core samples examined from the Woodford Shale zone (6666-6696 ft) are organic-rich shales. The sample from 6669.1 ft is a mixture of organic-rich shale and radiolarian chert. The samples contain varying amounts of siliceous and calcareous fossil debris. Small tabular mollusk fragments, crushed agglutinated foraminiferal tests (siliceous), radiolaria and conodonts are common. Detrital quartz silt is present in small amounts. Opaque, filamentous and dispersed kerogen occurs throughout the rock fabric of all three samples. Portions of the shale rock matrix contain microcrystalline silica and varying amounts of replacive pyrite.

Interlaminated Chert and Siliceous Shale (6669.1 Ft) - The 6669.1 ft sample consists of interlaminated siliceous shale and radiolarian chert. Cherty laminae are thin and interspersed with organic-rich shale laminae. Cherty laminae range from several millimeters to 1.5 cm in thickness. This rock contains small amounts of scattered terrigenous material. Silt and sand are scattered throughout the shaly portion of the sample. Mean grain size of terrigenous sand and silt = 0.01-0.02 mm. The cherty portion of the sample is laminated to microcrosslaminated. Bedding is much more clearly visible in the cherty laminae than in the more shaly portions of the sample. Skeletal debris and terrigenous components are commonly aligned parallel to laminae.

The rock matrix in cherty portions of the sample consists of a mixture of microcrystalline silica and organic-rich shale. The shaly portion of the sample is characterized by platy shale particles up to 5-10 μm in length and less than a few tenths of a micron thick. Small amounts of amorphous, filamentous kerogen are also present within the rock fabric. Detrital silt grains are disseminated throughout the shale matrix. Silt grains are angular in shape and consist predominantly of monocrystalline quartz.

Fossil debris is common in the cherty portion of the sample. Circular radiolarian tests are most abundant. Tests are highly altered and infilled by authigenic quartz, pyrite and dead oil. Small amounts of tabular skeletal debris are also present. Skeletal debris is highly altered and most fragments are also silicified. Silica is interpreted as having originated from the breakdown of siliceous microfossils.

This sample has low porosity and permeability. These siliceous shales lack primary intergranular or secondary dissolution porosity. The rock pore system consists entirely of micropores developed within silicified portions of the matrix augmented by sheet-like micropores developed between platy shale particles. Microporosity is also present within some silicified radiolarian tests. Partial silicification of portions of the matrix contributes to reduced porosity and permeability.

Organic-Rich Shale (6681.9 and 6690.9 Ft) - Rocks comprising this portion of the section are poorly sorted, very fine grained, organic-rich shales. The rocks are thinly to crudely laminated. Bioturbation is evident in both samples. Small shale and silt-filled

burrows are scattered throughout the rock fabric. The rocks consist of a groundmass of dispersed detrital shale supporting scattered detrital quartz silt grains and fossil debris as well as authigenic pyrite. The rock matrix consists of platy shale particles mixed with varying amounts of silica and carbonate material. Microcrystalline silica is far more abundant than detrital quartz in these rocks. Differential compaction is visible around pyrite crystals and silt-filled burrows.

The shale matrix supports scattered fossil debris and small amounts of detrital silt grains. Skeletal components include radiolaria, flattened agglutinated foraminifera, algal spores, conodonts and small tabular mollusk fragments. Detrital silt is less abundant than skeletal debris. The mean grain size for silt grains ranges from 0.01-0.03 mm. Small amounts of very fine sand are also present. Silt grains consist largely of monocrystalline quartz. Authigenic pyrite, formed prior to burial at the sediment/sea water interface by sulfate reducing bacteria, is a common component of these shales. Pyrite occurs both as framboidal masses and as aggregates of octahedral crystals that have grown displacively within the rock matrix. Pyrite also partially replaced some biotic constituents.

Organic-rich shales have low porosity and permeability. The rocks lack primary intergranular or secondary dissolution porosity. Natural shear fractures visible in the sample from 6681.9 ft are partially filled by carbonate minerals. Shear fractures are low-angle features and would likely be closed in the subsurface due to lithostatic stress. Porosity is restricted entirely to microporosity. Two types of micropores exist within these shales: 1) pores less than 1 μm in diameter developed within silicified portions of the matrix, and 2) slot-like micropores developed between platy shale particles. Slot-like micropores are typically oriented parallel to bedding resulting in a strong bedding parallel anisotropy to permeability.

Hunton Limestone

Thin section evaluation of ten (10) samples from the Hunton Limestone indicates that several Rock Types or lithofacies are present within the described section. These samples are divided into four (4) Rock Types or lithofacies: 1) highly dolomitized packstones and packstones to wackestones, 2) relatively undolomitized packstones, 3) undolomitized muddy packstones to wackestones, and 4) skeletal grainstones.

Dolomitized Packstones and Packstones to Wackestones

The upper portion of the Hunton Limestone section is characterized by partially dolomitized packstones and packstones to wackestones. This lithofacies is represented by six (6) samples (6696.5, 6700.1, 6705.2, 6710.2, 6720.2 and 6725.2 ft). These rocks are very dolomitic, but exhibit both remnant packstone and wackestone textures. Dolomitization has been selective and has preferentially affected more finely crystalline portions of the rock. The original micrite matrix is completely dolomitized. Small skeletal grains have also been dolomitized or removed through dissolution. The texture of several samples suggests interlamination of packstones and wackestones. Much of

the original limestone fabric has been obliterated. The original limestone fabric may have been similar to that of the undolomitized packstone or packstone to wackestone facies (Plate 8 and Plate 11). Compaction is moderate to severe and characterized by stylolites and interpenetrative grain-to-grain contacts.

Skeletal grains in this lithofacies are dominated by echinoderm fragments. Crinoid columnals, plates and spines are common. Small, tabular brachiopod fragments were also observed in several samples. These calcareous skeletal grains have been unaffected by the dolomitization process.

These rocks are moderately to heavily cemented. Common cements in this facies include euhedral dolomite, blocky pore filling calcite, syntaxial calcite overgrowths on echinoderm fragments and euhedral plagioclase. Coarse, euhedral dolomite commonly fills secondary and intraparticle pores (Plate 10B). Syntaxial calcite overgrowths are present on most echinoderm fragments. Syntaxial overgrowths formed early in the diagenetic history of this reservoir. These overgrowths form unit crystals with the echinoderm fragment and are also undolomitized. Blocky calcite formed relatively late in the diagenetic history of the reservoir. Blocky calcite fills intercrystalline and secondary pores. Small tabular plagioclase crystals are present throughout the pore system of these rocks. It could not be determined if these are overgrowths on silt-sized plagioclase grains or purely an authigenic cement. These rocks contain modest amounts of bitumen or dead oil. Bitumen fills or partially fills intercrystalline pores, secondary pores and fractures.

Porosity is moderately well developed in some samples from this lithofacies. Samples from the upper portion of the Hunton zone exhibit somewhat better porosity than those in the lower portion. Porosity within individual samples is patchily distributed. Some areas are tightly cemented, whereas other areas retain significant porosity. Dolomitization has resulted in the formation of modest amounts of intercrystalline macroporosity. Microintercrystalline porosity is present within finely crystalline dolomitized laminae. During the dolomitization process, secondary porosity was also produced. Carbonate grains (probably small skeletal fragments) were dissolved, leaving moldic pores. Several samples exhibit small amounts of fracture porosity and intraparticle porosity. Porosity measured for samples from this lithofacies ranges from 3.2-4.0% and permeability from 0.05-0.16 md. The low porosity and relatively low permeability measurements are consistent with the patchy distribution of porosity and the relative abundance of pore filling cements.

Relatively Undolomitized Packstones

The sample from 6716.2 ft is characterized as a relatively undolomitized packstone. Dolomitization in this sample has affected the former micritic matrix, but not skeletal components. As in the previous lithofacies, echinoderm fragments are the most abundant skeletal component. Crinoid plates, columnals and spines are abundant. Brachiopod fragments are present in minor amounts. Skeletal fragments are in grain

support. Void space between grains is filled by a mixture of dolomitized micrite matrix and calcite cement.

The rock fabric in this sample is heavily cemented (Plate 8A). The dolomitized matrix is composed of euhedral to subhedral dolomite crystals. Syntaxial calcite overgrowths are abundant. Most echinoderm fragments contain overgrowths. Blocky pore filling calcite cement is present in small amounts. Euhedral dolomite rhombs partially fill rare secondary pores. Individual rhombs range from 75-200 μm in diameter.

Intercrystalline macroporosity is poorly developed in this sample. The finely crystalline dolomitized matrix contains modest amounts of intercrystalline microporosity (Plate 8C). These pores are less than 5 μm in diameter and poorly interconnected. Rare secondary pores are present throughout the rock fabric. These pores are partially to totally filled by authigenic cements. Reservoir quality in this lithofacies is poor.

Undolomitized Muddy Packstones to Wackestones

The samples from 6735.5 and 6742.6 ft are characterized as muddy, skeletal packstones to wackestones. These samples exhibit minor or localized dolomitization. The sample from 6742.6 ft contains a karst related solution void filled by internal sediment and crystalline dolomite. The area immediately adjacent to the void is heavily dolomitized, but the remainder of the sample is not. Portions of these rocks are in grain support and portions are in mud support. The micrite matrix is the dominant component in these samples. Skeletal grains are relatively abundant and much more diverse than in the overlying, partially dolomitized rocks. Skeletal components include echinoderm plates and columnals, brachiopod fragments and spines, ostracods, bryozoans, trilobite fragments and spines, and small unidentified tabular fragments. Skeletal fragments are angular and poorly sorted (Plate 11A).

These rocks contain less authigenic cement than the previous two (2) lithofacies. Micrite matrix fills many interparticle voids. Syntaxial calcite overgrowths are present on echinoderm fragments. Small amounts of calcite fill secondary pores. Euhedral dolomite crystals partially replace carbonate grains and the rock fabric. Tabular plagioclase crystals are present in some portions of the samples.

Porosity in these rocks is poorly developed. A relatively large solution void is present in the sample from 6742.6 ft. This void is partially filled by internal sediment and coarsely crystalline dolomite. Examination of the core from this zone indicates that a high angle, open fracture is also present. The fracture has limited vertical extent, but is lined by euhedral dolomite crystals, indicating that it is open in the subsurface. Microporosity is the dominant porosity type in this zone. Microporosity is present within the micrite matrix in both samples. Microporosity is also present within selected skeletal grains in the sample from 6742.6 ft. Micropores are less than 5 μm in diameter and poorly interconnected. Measured porosity for the 6735.5 ft sample = 0.6% and permeability = 0.004 md. Matrix reservoir quality in this facies is poor. High angle, open fractures may provide some localized porosity and permeability.

Skeletal Grainstones

The 6750.2 ft sample is characterized as a skeletal grainstone. This sample is from a thin, grain-rich zone between 6749.5-6751.5 ft. The rock fabric is in grain support and heavily cemented by sparry calcite. Skeletal carbonate grains are abundant. Non-skeletal grains are also present in lesser amounts. Common skeletal components include green algae, algal coated grains, echinoderm fragments, brachiopod fragments and spines, bryozoans and trilobites. Non-skeletal grains are a mixture of ooids, intraclasts and small muddy peloids.

Sparry pore filling calcite is the most abundant cement in this lithofacies. Virtually all interparticle voids are filled by calcite spar. Syntaxial calcite overgrowths are present on echinoderm fragments. Some skeletal grains and portions of the rock fabric are partially replaced by microporous silica. Minor amounts of euhedral dolomite partially replace some skeletal grains (algal grains more abundantly than other skeletal components). Small euhedral plagioclase crystals are scattered throughout the sample.

Interparticle pores in this lithofacies are completely occluded by calcite cement. No macroporosity is visible in the rock fabric. Microporosity is present within silicified areas (Plate 13A). Microporosity is also present within some skeletal grains. Skeletal grains were affected by endolithic algae shortly after deposition. These algae have created microporosity within the grain structure. Micropores are isolated within grains and poorly interconnected (Plate 13C). Measured porosity for this sample = 1.7% and permeability = 0.007 md. Reservoir quality is poor.

2.4 X-Ray Diffraction Analysis

Bulk x-ray diffraction analysis was performed on six (6) samples from the Hunton Limestone zone. XRD samples correspond to samples used in routine core analysis. These samples are dominated by carbonate minerals. No clay was detected in any of the analyzed samples. Calcite is the most abundant mineral phase present in these rocks. Calcite abundance ranges from 49-92%. Dolomite is second in abundance (8-50% of the bulk composition). Small amounts of quartz (trace-7%) and plagioclase (trace) are also present. Quartz and plagioclase are both authigenic components and generally do not occur as detrital grains.

Table 2.1
Analyses Performed
Sedna Energy - Fowler No. 2-17 Well

DEPTH Ft	SAMPLE TYPE	SAMPLE CONDITION	FORMATION/ ZONE	TS	BULK XRD	SEM/ EDS	ROUTINE φ, K	SCAL
6669.1	CCS	Good	Woodford Shale	X				
6681.9	CCS	Good	Woodford Shale	X				
6690.9	CCS	Good	Woodford Shale	X				
6696.5	CCS	Good	Hunton Limestone	X				
6700.1	CCS	Good	Hunton Limestone	X				
6705.2	CCP	Good	Hunton Limestone	X	X			
6710.2	CCP	Good	Hunton Limestone	X	X			
6716.2	CCS	Good	Hunton Limestone	X				
6720.2	CCP	Good	Hunton Limestone	X	X			
6725.2	CCP	Good	Hunton Limestone	X	X			
6735.5	CCP	Good	Hunton Limestone	X	X			
6742.6	CCS	Good	Hunton Limestone	X				
6750.2	CCP	Good	Hunton Limestone	X	X			

CCP Conventional Core Plug RSWC Rotary Sidewall Core
 CCS Conventional Core Sample CT Cuttings
 SWC Percussion Sidewall Core OT Other

Table 2.2
Thin Section Analysis
Sedna Energy - Fowler No. 2-17 Well

DEPTH Ft	RESERVOIR ZONE	LITHOLOGY	COMPOSITION	PORE FILL/AUTHIGENIC CEMENTS	PORE TYPES	COMPACTION
6669.1	Woodford Shale	Organic-rich shale	Abundant depositional shale, modest amounts of dispersed and laminar organic matter, thin beds of radiolarian chert, minor calcareous and terrigenous debris	Depositional shale matrix, silicification of thin radiolaria beds, infilling of tests by silica, partial replacement of the rock fabric and tests by pyrite and bitumen	Microporosity in the shale matrix and within silicified biotic fragments.	Moderate, differential compaction around more rigid structures
6681.9	Woodford Shale	Organic-rich, calcareous shale	Abundant depositional shale matrix, scattered calcareous fossil fragments, minor terrigenous sand and silt, rare conodonts, siliceous microfossils, algal spores, dispersed organic matter	Fracture filling calcite, replacive pyrite, silica replacement of skeletal fragments	Microporosity within the matrix	Moderate compaction, shear fractures
6690.9	Woodford Shale	Very organic-rich shale	Depositional shale matrix, scattered terrigenous grains, conodonts, algal spores, phosphatic grains, wispy and dispersed organic matter	Euhedral dolomite replacement of the fabric, minor silicification of skeletal grains, minor pyrite	Microporosity in the matrix and associated with silicified grains	Moderate, differential compaction around burrows
6696.5	Hunton Limestone	Partially dolomitized echinoderm packstone	Crinoid columnals and plates, rare terrigenous grains	Extensive dolomitization of the finely crystalline matrix, pore filling euhedral dolomite, pore filling blocky calcite, syntaxial overgrowths on echinoderms, pore filling megaquartz	Molds/dissolution pores, intercrystalline macroporosity and microporosity, narrow fractures	Moderate compaction in fossil-rich laminae, early cementation
6700.1	Hunton Limestone	Partially dolomitized echinoderm packstone/wackest one	Crinoid columnals, plates and spines, rare brachiopod fragments	Extensive dolomitization of the muddy matrix, euhedral pore filling dolomite, pore filling calcite, syntaxial overgrowths on echinoderm fragments, euhedral plagioclase, pore filling bitumen	Microintercrystalline porosity in the dolomitized matrix, intercrystalline macropores, remnant molds/dissolution pores,	Moderate to severe, stylolites
6705.2	Hunton Limestone	Partially dolomitized echinoderm packstone/wackest one	Crinoid columnals and plates, minor brachiopod fragments, rare quartz and plagioclase grains	Selective dolomitization of the matrix, euhedral pore filling dolomite, pore filling calcite, syntaxial overgrowths on echinoderm fragments, euhedral plagioclase overgrowths, pore filling bitumen	Intercrystalline macroporosity and microporosity, rare dissolution pores/molds, narrow (<5µ aperture) fractures	Moderate compaction, early cementation in some zones
6710.2	Hunton Limestone	Partially dolomitized echinoderm packstone	Echinoderm plates, columnals and spines, brachiopod and bryozoan fragments	Minor dolomitization of the matrix, euhedral dolomite in secondary pores, patchy calcite pore filling, syntaxial overgrowths, euhedral plagioclase, pore filling bitumen	Intercrystalline macroporosity, partially cemented secondary pores, microporosity in the finely crystalline matrix	Moderate compaction, especially in dolomitized laminae

Table 2.2 (Cont)

Thin Section Analysis
Sedna Energy Fowler No. - 2-17 well

DEPTH Ft	RESERVOIR ZONE	LITHOLOGY	COMPOSITION	PORE FILL/CEMENTS	PORE TYPES	COMPACTION
6716.2	Hunton Limestone	Relatively undolomitized echinoderm packstone	Echinoderm plates and columnals, brachiopod fragments, possible dolomitized peloids	Euhedral dolomite in secondary pores, syntaxial overgrowths on echinoderm fragments, pore filling calcite, dolomitization of the finely crystalline matrix	Microporosity in the matrix, small molds/vugs	Moderate compaction, early cementation
6720.2	Hunton Limestone	Partially dolomitized, echinoderm packstone and wackestone	Echinoderm fragments, whole and fragmented brachiopods	Selective dolomitization, pore filling dolomite, pore filling calcite, syntaxial calcite overgrowths on echinoderm fragments, euhedral plagioclase, abundant pore filling bitumen	Partially cemented molds, intercrystalline macropores and micropores, high angle fractures	Moderate to severe in undolomitized laminae
6725.2	Hunton Limestone	Partially dolomitized, interlaminar packstone and wackestone	Echinoderm fragments, rare brachiopod fragments	Syntaxial calcite overgrowths on echinoderm fragments, blocky pore filling calcite, euhedral dolomite, euhedral plagioclase, pore filling bitumen	Large molds/vugs, intercrystalline macropores, micropores in finely crystalline laminae, irregular, moderate angle fractures	Moderate compaction in packstone laminae
6735.5	Hunton Limestone	Muddy skeletal packstone to wackestone	Brachiopod spines and fragments, echinoderm fragments, ostracods, bryozoans, trilobite plates and spines, small tabular fragments	Syntaxial calcite overgrowths on echinoderm fragments, sparse euhedral dolomite crystals, pore filling calcite, plagioclase, recrystallization of micrite to microspar	Microporosity in the muddy matrix, rare partially filled molds	Moderate in some laminae
6742.6	Hunton Limestone	Partially dolomitized muddy skeletal packstone	Echinoderm plates and spines, productid brachiopods, ostracods, trilobites, sponge spicules	Selective dolomitization around the perimeter of karst voids, void filling euhedral dolomite, replacive pyrite, pore filling calcite	Molds, microporosity within some carbonate grains, rare high angle fractures	Moderate
6750.2	Hunton Limestone	Skeletal grainstone	Echinoderm plates and spines, green algal fragments, algal coated grains, brachiopods, trilobites, ooids, intraclasts, brachiopods	Abundant pore filling calcite, syntaxial calcite overgrowths, minor silicification of the matrix, partial dolomitization of selected grains, euhedral plagioclase	Microporosity within silicified areas and some carbonate grains (algal grains)	Minor compaction, early cementation

Table 2.3
X-Ray Diffraction Analysis
Sedna Energy - Fowler No. 2-17 WELL

SAMPLE DEPTH (Ft)	OTHER MINERALS						CARBONATE MINERALS					DRILLING MUD SOLIDS				TOTALS			
	QUARTZ	K-FELDSPAR	PLAGIOCLASE	PYRITE	APATITE	OTHER	ANKERITE	CALCITE	DOLOMITE	SIDERITE	OTHER CARBONATES	BENTONITE	HALITE	BARITE	OTHER SOLIDS	TOTAL CLAY MINERALS	TOTAL OTHER MINERALS	TOTAL CARBONATES	TOTAL DRILL SOLIDS
6705.2	Tr		Tr					62	38						0	Tr	100	0	
6710.2	Tr		Tr					54	46						0	Tr	100	0	
6720.2	Tr		Tr					57	43						0	Tr	100	0	
6725.2	1							49	50						0	1	99	0	
6735.5	Tr							92	8						0	Tr	100	0	
6750.2	7							79	14						0	7	93	0	

3.0 WELLSITE FIELD SERVICES AND DESORPTION

3.1. Introduction and Procedures

Calculating a reliable estimate of a reservoir's gas in place requires the input of accurate and complete gas content data. The data should be obtained using methods specific to unconventional gas reservoirs and taken by experienced laboratory personnel. Appropriate sampling procedures specific to the formation type, and proper sample handling of the recovered core in the field, are critical for determination of the in situ sorbed gas content in coals or gas shales. This is especially essential for construction of a cumulative gas curve that will give an accurate extrapolation of the lost gas component back to time zero.

Total gas content is the summation of three components: lost gas - from data collected at wellsite, desorbed gas - initially measured in the field and completed in the lab, and residual gas - lastly determined in the lab. Lost gas is estimated by projecting the first 24 hour's worth of cumulative desorption volumes back to the point at which desorption began before the core was brought to surface. Desorption measurements begin at the wellsite and continue for several weeks in the lab until waning volumes, change in gas composition data or customer preference indicate that the accumulated gas volume data is sufficient, and so further analysis of the core may commence. Residual gas is the final component of total gas content, measured by crushing the coal at the end of desorption, as rapidly as possible after the canisters are opened.

Westport Technology Center was requested to perform Wellsite Desorption and determine total gas content on shale recovered from the Fowler #2-17 well in Haskell County, Oklahoma.

Shale was recovered from the Fowler #2-17 well at a depth of 6672.00ft – 6696.0ft. Once the shale arrived at the surface of the well, it was laid out to be marked for depths. The shale was quickly enclosed in air tight sealed canisters to minimize lost gas and exposure to oxidation or desiccation. Table 1.1 below illustrates an inventory of the shale that was recovered.

Shale canisters were set up at the wellsite field laboratory at a constant reservoir temperature in thermostatically controlled water baths. Volumetric gas readings immediately began on all shale canisters and continued around the clock for at least 24 hours until desorbed volumes reduced to a level allowing for less frequent measurements. Desorbed gas volume, time, date, canister temperature, air temperature, and barometric pressure were recorded for every sample at each reading. The canisters were then transported in the wellsite desorption trailer to Westport Technology Center where readings continued at reservoir temperature in the laboratory.

3.2 Results

A summary of the complete shale analysis is compiled below in Table 3.2 Summary of Shale Gas Properties. The lost gas component of total gas content as determined from wellsite data, is listed as a separate column.

Gas contents, gross basis of the samples range from 161.4 to 281.3 SCF/ton for the Fowler #2-17 well.

Table 3.1. Inventory of Recovered Coal and Canisters

Canister ID	Depth (ft)	Well Name
1	6696.0	Fowler #2-17
2	6692.0	Fowler #2-17
3	6688.0	Fowler #2-17
4	6684.0	Fowler #2-17
5	6680.0	Fowler #2-17
6	6676.0	Fowler #2-17
7	6672.0	Fowler #2-17

Table 3.2. Summary of Shale Gas Properties

Canister ID	Depth (ft)	Well Name	Temperature (°F)	"As Received" Weight (g)	Canister Headspace Volume (cm ³)	Gas Content Gross Basis (SCF/ton)	Linear Lost Gas (cc)	Residual Gas (SCF/ton)	Total Gas Content (cc)
1	6696.0	Fowler #2-17	61.0	5020	480	161.4	18.2	3.1	4570.9
2	6692.0	Fowler #2-17	61.0	4620	120	183.9	114.4	4.1	5209.4
3	6688.0	Fowler #2-17	61.0	6160	160	281.3	106.6	5.9	7969.2
4	6684.0	Fowler #2-17	61.0	5260	20	196.1	70.5	4.4	5555.7
5	6680.0	Fowler #2-17	61.0	4500	180	226.2	133.4	6.7	6408.7
6	6676.0	Fowler #2-17	61.0	5020	520	189.0	107.6	5.9	5354.1
7	6672.0	Fowler #2-17	61.0	5060	640	167.2	91.4	4.1	4736.7

4.0 LABORATORY DESORPTION

4.1 Long-Term Desorption

Total gas content is the summation of three components: lost gas, desorbed gas, and residual gas. Desorption measurements begin at the wellsite, and once the lost gas component has been obtained from constant measurements in the field, long-term desorption is completed in the laboratory. In the lab, while desorbing gas volumes are still elevated, readings are taken from the canisters twice daily. Toward the later half of long term desorption, readings are only necessary once a day or every 2 days. Canister samples are maintained in a bath at constant reservoir temperatures throughout gas desorption. Desorbed gas volumes are corrected for changes in barometric pressure and atmospheric temperature.

Shale samples from the Fowler #2-17 well were obtained and long term desorption was measured for approximately 3 months.

4.2 Headspace

At the end of laboratory desorption, canisters were opened one at a time to measure headspace volume and residual gas. Mass of the shale, canister and water were recorded, and canister air headspace was determined by gravimetric liquid replacement. Masses are taken for the purpose of calculating total gas content in scf/ton, while void volume corrects the total gas content for environmental conditions.

4.3 Residual Gas

Residual gas is the third and final component of the total gas content of a sample. Residual gas measurements were taken at once upon opening each canister to minimize exposure to air, prevent moisture loss, oxidation, and unmeasured gas loss. Samples were maintained as close to reservoir temperature as possible during the transfer process and during residual gas measurements. Removing samples from the high methane / carbon dioxide atmosphere in the sealed canister also accelerates the loss of any remaining carbon based gas, so subsampling is done rapidly and remaining sample is resealed.

Each section of shale was split into representative whole subsamples of approximately 30 grams, and crushed in a sealed chamber equipped with a one-way valve for simultaneous measurement of evolved gas. Gas evolved is measured by liquid displacement using a burette. The measurement was repeated three times with preweighed subsamples and then averaged for the reported residual gas value.

4.4 Results

The previous Table 3.2 presents the Summary of Shale Gas Properties. The table breaks down total gas content by desorbed gas, residual gas, and lost gas for each

sample. Total gas volumes are also given in Table 3.2. Gas volumes, desorbed for each sample, are described in desorption curves in Figures 4.1 – Figure 4.7 below as cumulative volume over the inverse of time. Gas contents, gross basis of the samples range from 161.4 – 281.3 SCF/ton for the Fowler #2-17 well.

All shale sections had canister headspace and mass measured. All 7 of the samples were evaluated for residual gas analysis. Residual gas data is also presented in Table 3.2. Residual gas of the samples range from 3.1 – 6.7 SCF/ton.

All individual sample data is located in Appendix D.

Figure 4.1. Cumulative Gas Desorbed, Canister #1

Company: Sedna Energy
Well Name: Fowler #2-17
Location: Haskell County, Oklahoma

Canister Number: 1
Seam Identification: Woodford
Top of test interval (ft): 6696.00
Btm of test interval (ft):
Interval Thickness (ft): 1.00

Cumulative Gas Desorped vs. Time

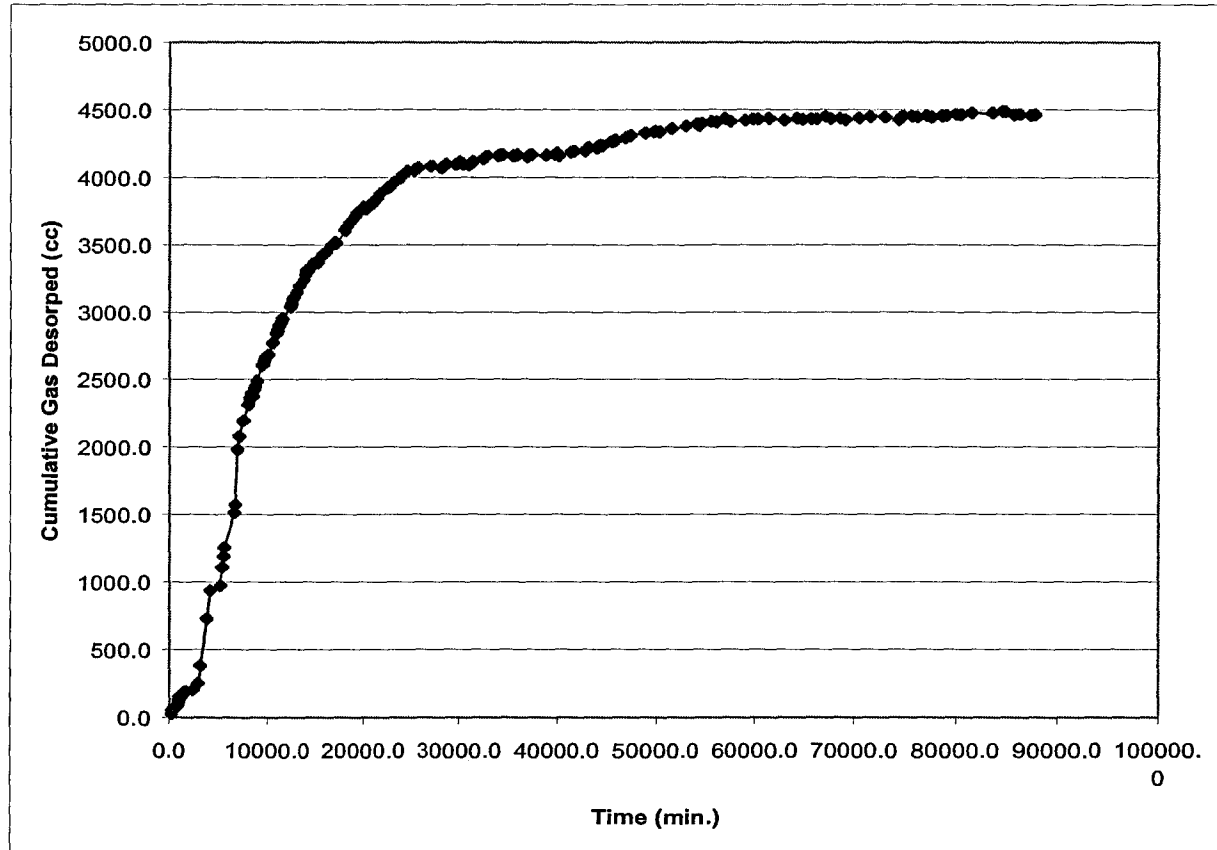


Figure 4.2 Cumulative Gas Desorbed, Canister #2

Company: Sedna Energy
Well Name: Fowler #2-17
Location: Haskell County, Oklahoma

Canister Number: 2
Seam Identification: Woodford
Top of test interval (ft): 6692.00
Btm of test interval (ft):
Interval Thickness (ft): 1.00

Cumulative Gas Desorbed vs. Time

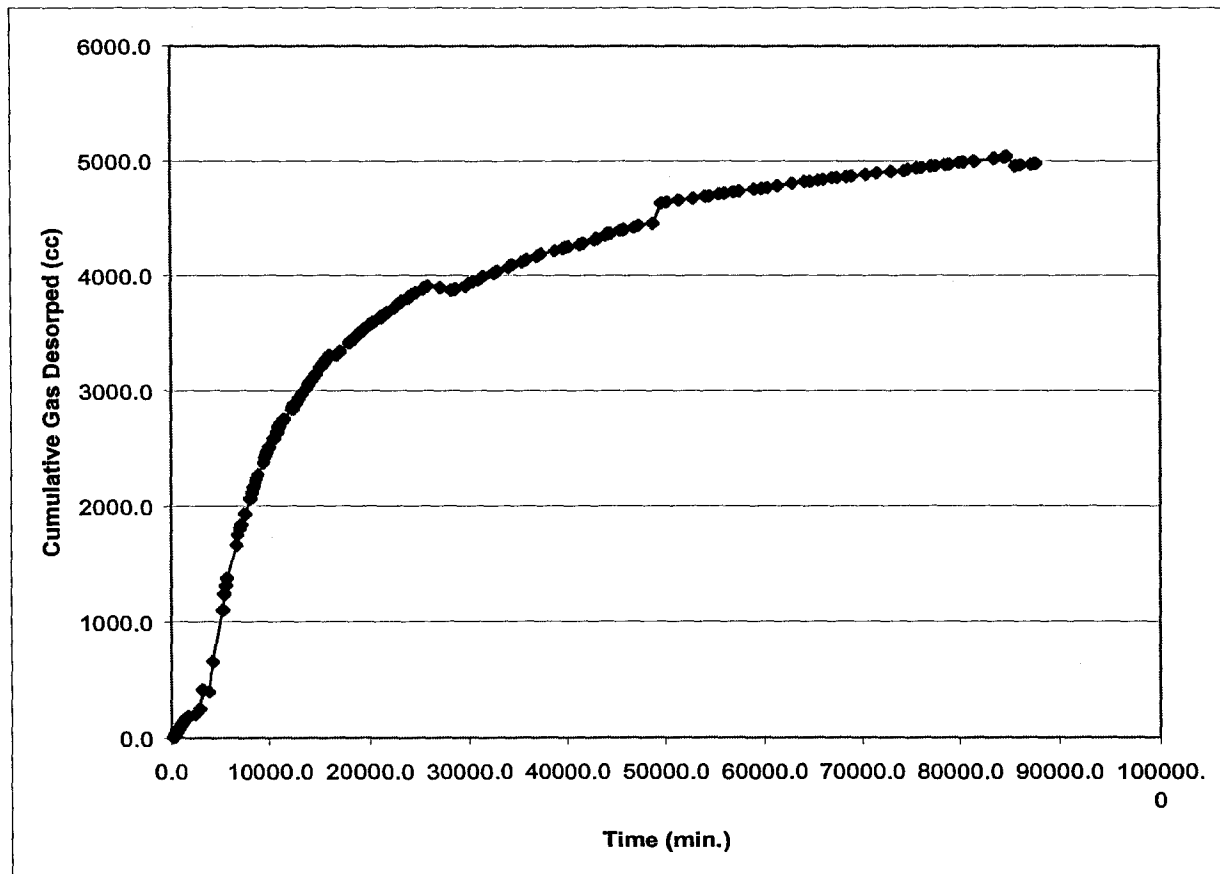


Figure 4.3 Cumulative Gas Desorbed, Canister #3

Company: Sedna Energy
Well Name: Fowler #2-17
Location: Haskell County, Oklahoma

Canister Number: 3
Seam Identification: Woodford
Top of test interval (ft): 6688.00
Btm of test interval (ft):
Interval Thickness (ft): 1.00

Cumulative Gas Desorbed vs. Time

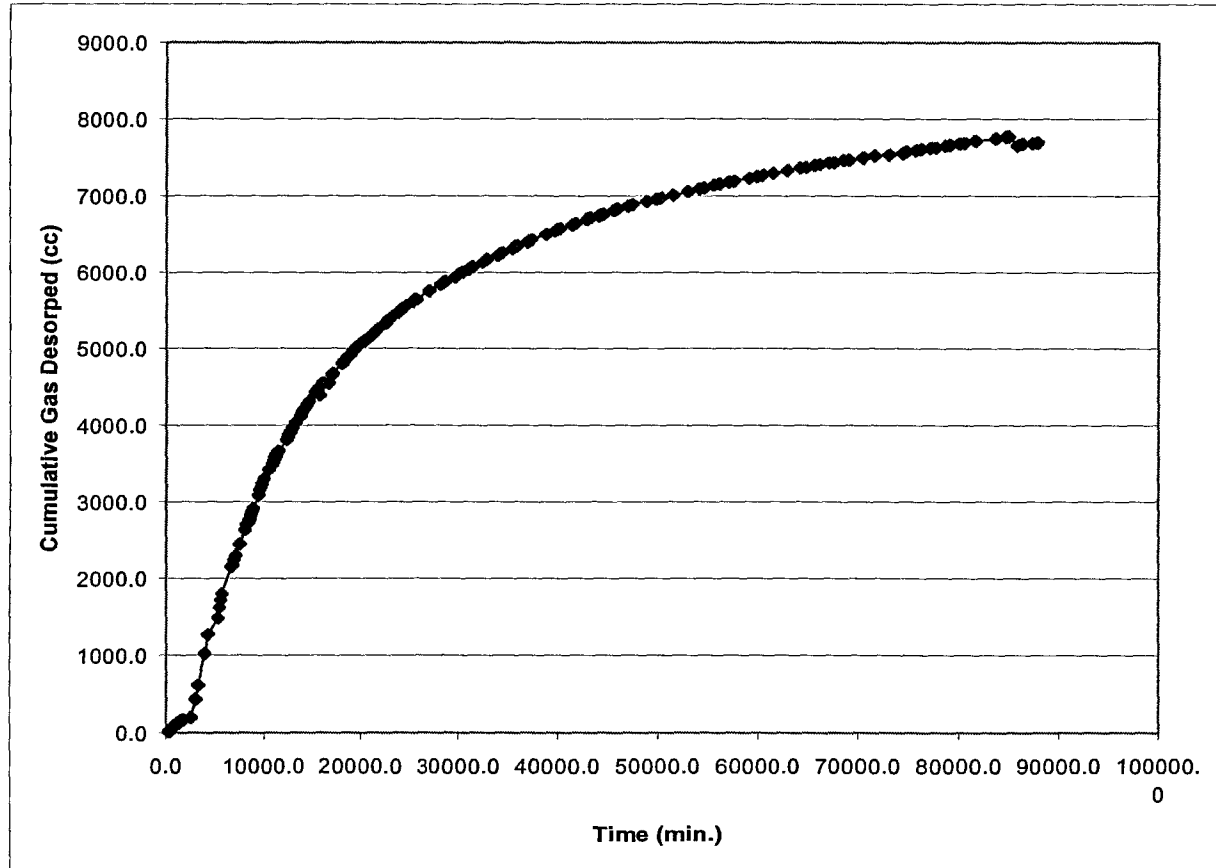


Figure 4.4 Cumulative Gas Desorbed, Canister #4

Company: Sedna Energy
Well Name: Fowler #2-17
Location: Haskell County, Oklahoma

Canister Number: 4
Seam Identification: Woodford
Top of test interval (ft): 6684.00
Btm of test interval (ft):
Interval Thickness (ft): 1.00

Cumulative Gas Desorbed vs. Time

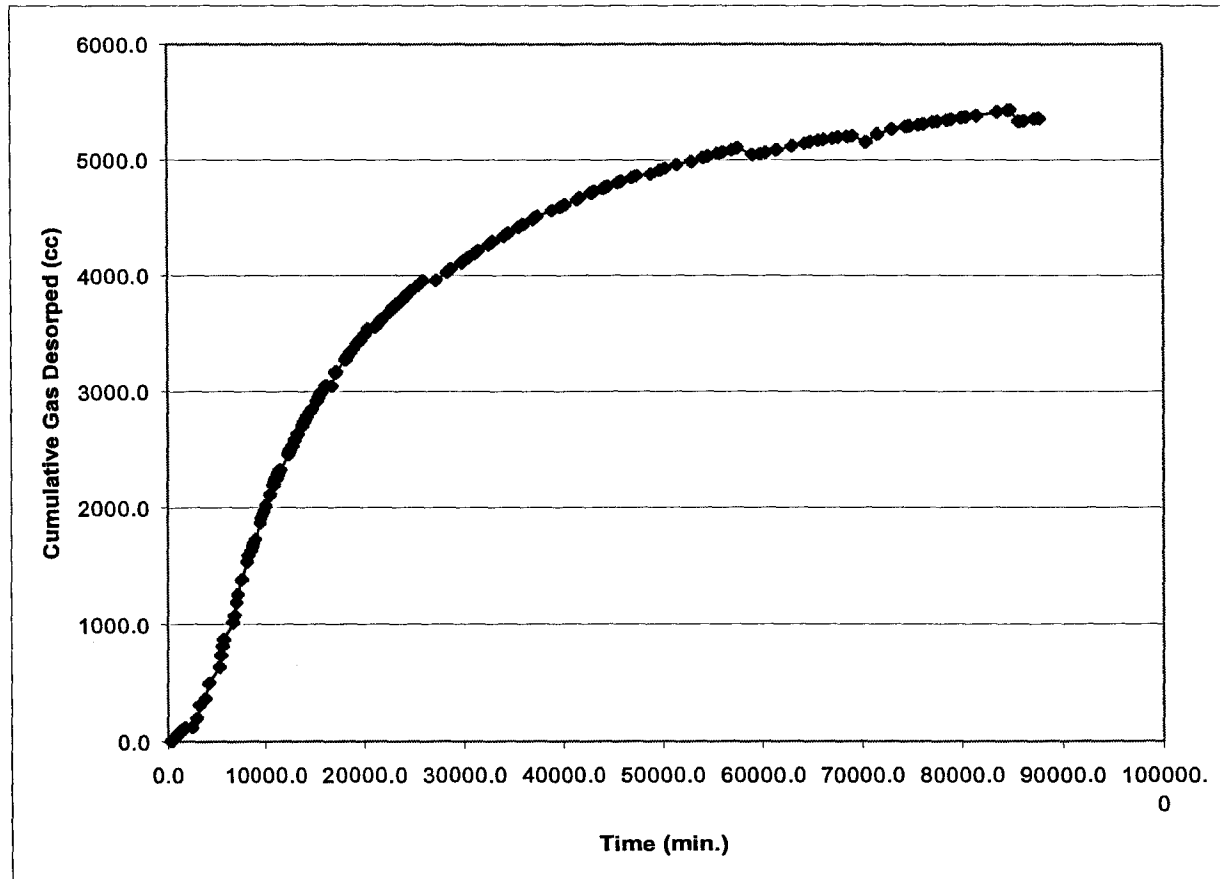


Figure 4.5 Cumulative Gas Desorbed, Canister #5

Company: Sedna Energy
Well Name: Fowler #2-17
Location: Haskell County, Oklahoma

Canister Number: 5
Seam Identification: Woodford
Top of test interval (ft): 6680.00
Btm of test interval (ft):
Interval Thickness (ft): 1.00

Cumulative Gas Desorbed vs. Time

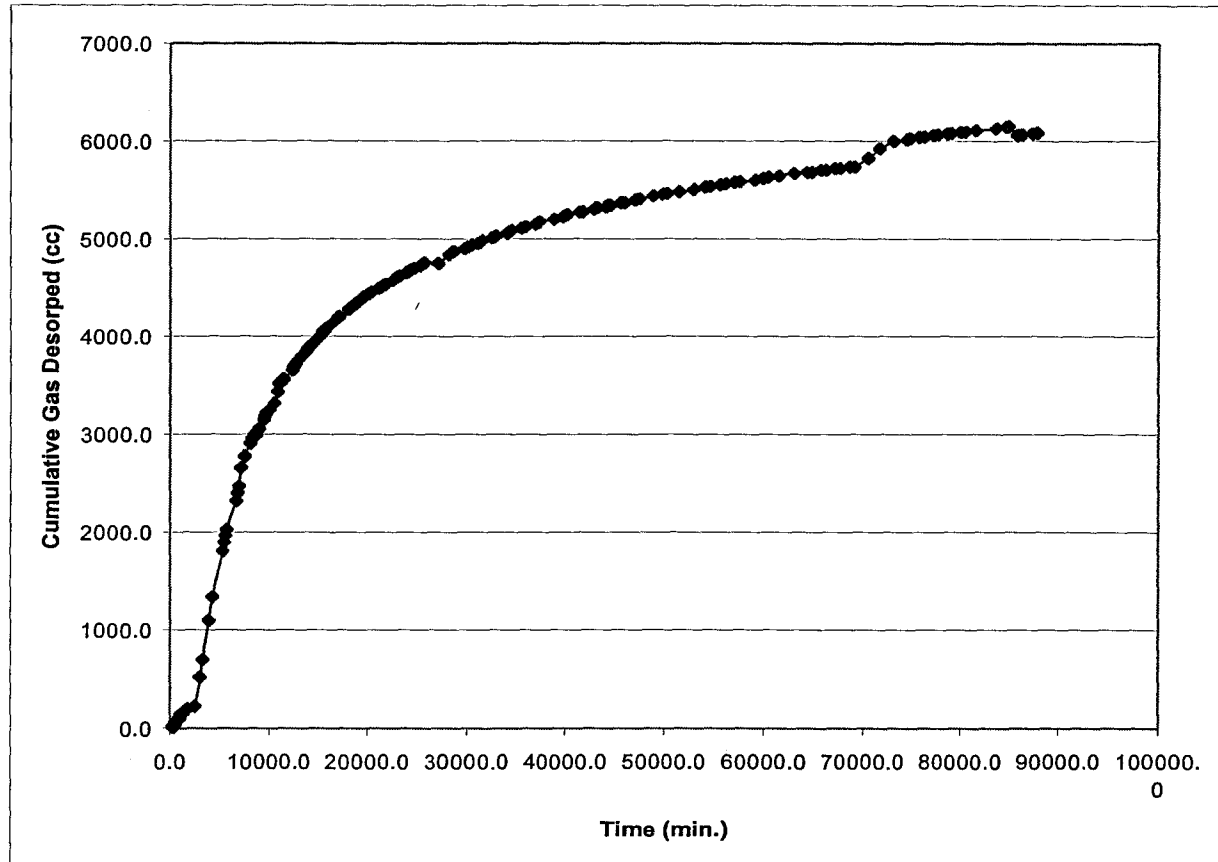


Figure 4.6 Cumulative Gas Desorbed, Canister #6

Company: Sedna Energy
Well Name: Fowler #2-17
Location: Haskell County, Oklahoma

Canister Number: 6
Seam Identification: Woodford
Top of test interval (ft): 6676.00
Btm of test interval (ft):
Interval Thickness (ft): 1.00

Cumulative Gas Desorbed vs. Time

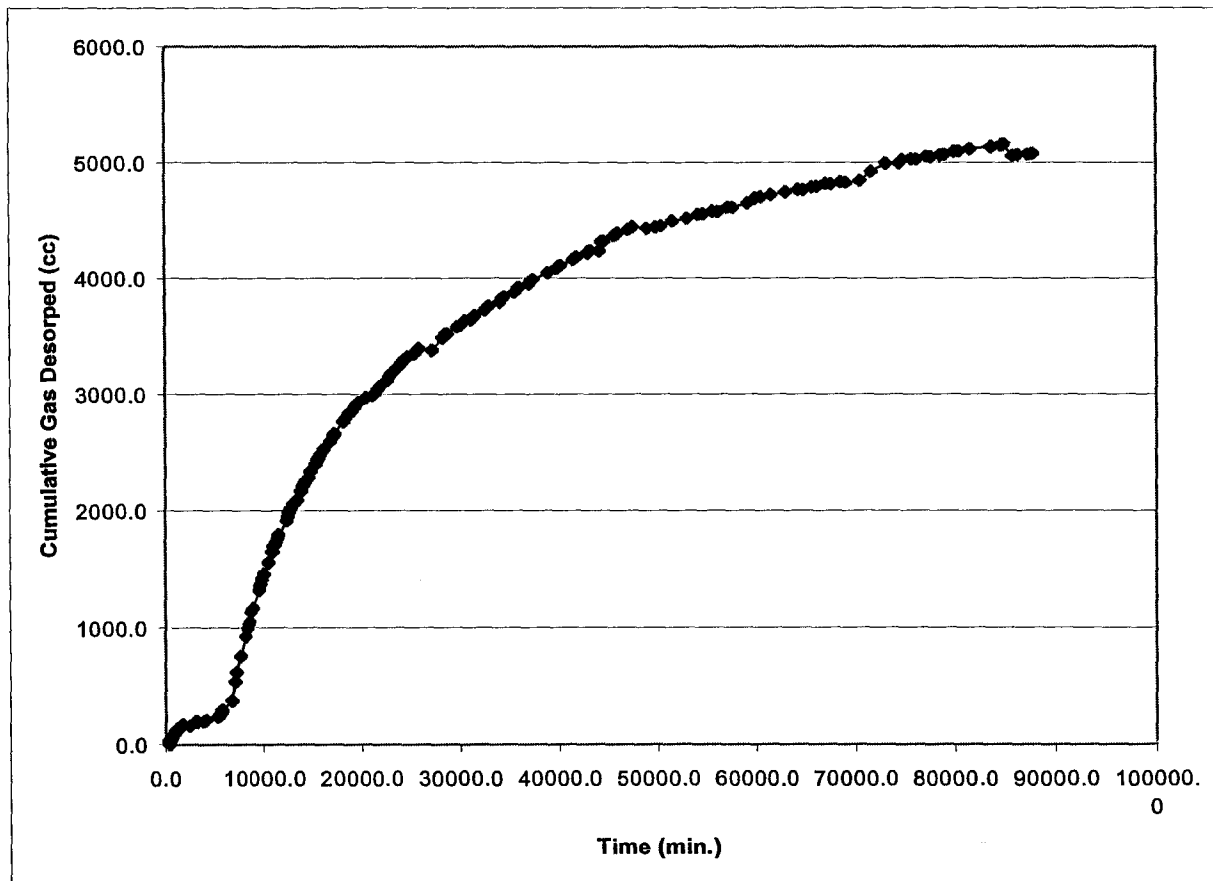
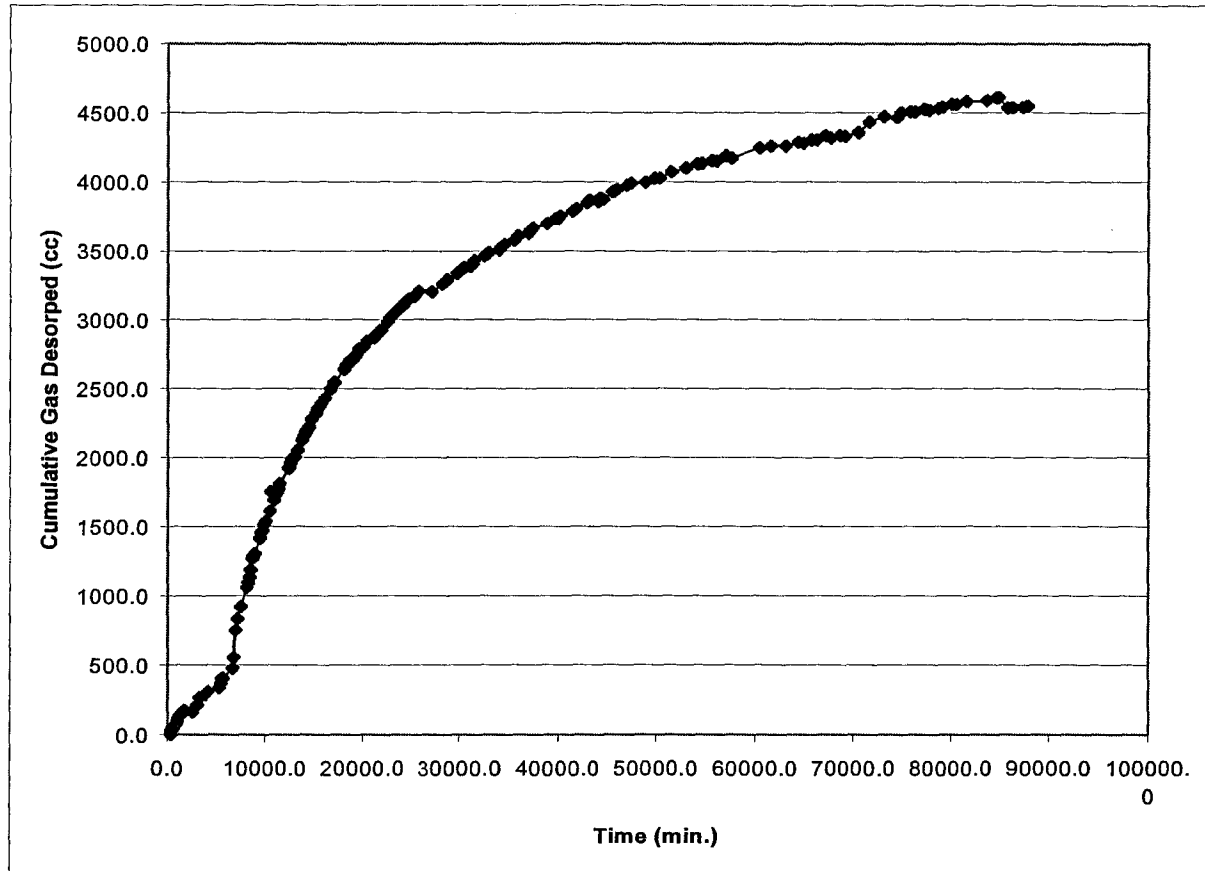


Figure 4.7 Cumulative Gas Desorbed, Canister #7

Company: Sedna Energy
Well Name: Fowler #2-17
Location: Haskell County, Oklahoma

Canister Number: 7
Seam Identification: Woodford
Top of test interval (ft): 6672.00
Btm of test interval (ft):
Interval Thickness (ft): 1.00

Cumulative Gas Desorbed vs. Time



5.0 TOTAL ORGANIC CARBON (TOC) AND ROCK EVAL

5.1 Introduction and Procedures

TOC (Total organic Carbon) in a rock is measured by combustion of a carbonate free rock sample in LECO carbon analyzer at high temperature (about 1200°C)

Rock-Eval analysis involves thermally distilling (300 degree C) free hydrocarbons (any remaining oil and gas) out of rock followed by heating to high temperature (600 C) to crack the remaining organic matter, often referred to as kerogen. Kerogen is organic matter that is insoluble in organic solvents and acids. It represents the remaining potential of the rock to generate hydrocarbons should it be exposed to higher temperatures than it was exposed to at any time in the past. If a source rock is highly mature, this remaining potential will be very low compared to its original potential due to hydrocarbon generation. Rock-Eval analysis provides the following data:

- * S1: free oil and gas content in mg HC/g rock
- * S2: remaining hydrocarbon potential in mg HC/g rock
- * Tmax: the pyrolysis temperature at which the maximum yield of S2 hydrocarbons occurs; an indication of thermal maturity-correlated to vitrinite reflectance
- * S3: organic carbon dioxide in mg CO₂/g rock; used for kerogen type assessment

Various ratios and values are also computed from TOC and Rock-Eval data to further characterize the maturity, kerogen type, and residual oil content (i.e., Tmax, HI, OI, S1/TOC and PI).

A detailed TOC & Rock-Eval analysis was outsourced to Humble Geochemical Services and performed on all 7 shale samples.

5.2 Results

The TOC and Rock-Eval Data Report Summary is listed in the below table. The remaining individual tables and charts are located in Appendix E.

Table 5.1. TOC and Rock Eval Data Report

TOC & Rock Eval Data Report Fowler #2-17 Well, Sedna Energy																		
HGS No.	Operator	Well Name	Client ID 1	Sample Type	Leco TOC	S1	S2	S3	Tmax (°C)	Calc. %Ro	HI	OI	S2/S3	S1/TOC	PI	Notes		
																Checks	Pyrogram	
06-4104-162612	Sedna Energy	Fowler #2-17	WTC-06-00009410001	ground rock	5.65	1.51	0.28	0.05	427 *	0.53	5	1	6	27	0.84	c, lc	f	
06-4104-162613	Sedna Energy	Fowler #2-17	WTC-06-00009410002	ground rock	7.07	0.90	0.30	0.07	531 *	2.40	4	1	4	13	0.75		f	
06-4104-162614	Sedna Energy	Fowler #2-17	WTC-06-00009410003	ground rock	7.52	0.85	0.32	0.06	531 *	2.40	4	1	5	11	0.73		f	
06-4104-162615	Sedna Energy	Fowler #2-17	WTC-06-00009410004	ground rock	5.09	0.93	0.23	0.10	527 *	2.33	5	2	2	18	0.80	lc	f	
06-4104-162616	Sedna Energy	Fowler #2-17	WTC-06-00009410006	ground rock	4.88	1.18	0.25	0.10	319 *	-1.00	5	2	3	24	0.83		f	
06-4104-162617	Sedna Energy	Fowler #2-17	WTC-06-00009410007	ground rock	8.98	1.01	0.22	0.07	316 *	-1.00	2	1	3	11	0.82		f	
06-4104-162618	Sedna Energy	Fowler #2-17	WTC-06-00009410008	ground rock	4.02	2.29	0.33	0.13	364 *	-1.00	8	3	3	57	0.87	c, lc	f	

<p>Note: "-1" indicates not measured or meaningless ratio</p> <p>* Tmax data not reliable due to poor S2 peak</p> <p>TOC = weight percent organic carbon in rock S1, S2 = mg hydrocarbons per gram of rock S3 = mg carbon dioxide per gram of rock Tmax = °C</p>	<p>HI = hydrogen index = S2 x 100 / TOC OI = oxygen index = S3 x 100 / TOC S1/TOC = normalized oil content = S1 x 100 / TOC PI = production index = S1 / (S1+S2) Calculated %Vro = 0.0180 x Tmax - 7.16 (Jarvie et al., 2001) Measured %Ro = measured vitrinite reflectance</p>	<p>Notes: c = Rock-Eval analysis checked and confirmed lc = Leco TOC analysis checked and confirmed</p> <p>Pyrogram: n=normal ‡S2sh = low temperature S2 shoulder ‡S2p = low temperature S2 peak †S2p = high temperature S2 peak f = flat S2 peak na = printer malfunction pyrogram not available</p>
---	--	---

6.0 EXTENDED GAS ANALYSIS

6.1 Introduction and Procedures

Gas composition is an important part of understanding a reservoir's total gas content. Other natural gas products of the coalification process besides methane are CO₂, N₂, H₂O and heavier Hydrocarbons. The quality of gas desorbed can change over time, due to the different adsorption affinities of each gas component. Initial gas compositions are higher in methane and heavier hydrocarbons when a coal seam is still at high pressure when beginning to desorb. Later in long term desorption, at lower pressures, CO₂ levels can be 50% of the gas content, which lowers the market value of the produced gas. Gas composition can also indicate whether the reservoir is mostly biogenic or thermogenic sources, and whether there is bacterial contamination of the samples.

6.2 Results

The extended gas analysis was performed on all seven shale samples at early, mid and late stages in the desorption process. Each sample was taken weekly for a total of seven weeks.

Individual sample data is located in Appendix F.